Tunable high-frequency magnetostatic waves in Thue-Morse antiferromagnetic multilayers

X. F. Zhang and R. W. Peng[a)]
National Laboratory of Solid State Microstructures, Nanjing University, Nanjing 210093, China and Department of Physics, Nanjing University, Nanjing 210093, China

S. S. Kang
Center for Materials for Information Technology, The University of Alabama, Tuscaloosa, Alabama 35487

L. S. Cao, R. L. Zhang, Mu Wang, and A. Hu
National Laboratory of Solid State Microstructures, Nanjing University, Nanjing 210093, China and Department of Physics, Nanjing University, Nanjing 210093, China

(Received 23 January 2006; accepted 11 June 2006; published online 28 September 2006)

We theoretically studied the magnetostatic excitation in self-similar antiferromagnetic(AF)/nonmagnetic(NM) multilayers, where the AF and NM layers were arranged in a Thue-Morse sequence. The dispersion relation of magnetostatic spin waves and the precession amplitude of the total magnetization were achieved. It is shown that the distribution of eigenfrequencies possesses two bands of dual structures and each subband presents a hierarchical feature. The states in the finite system can be categorized to three types: critical states in the subband, extended states in the band, and localized surface states in the gaps. The multiformity in frequency spectra leads to the tunable magnetostatic wave, which may have potential applications in designing devices of magnetostatic waves for microwave communications. © *2006 American Institute of Physics*.
[DOI: 10.1063/1.2335671]

I. INTRODUCTION

In recent years, much attention has been paid to magnetostatic (MS) excitations in artificial materials.[1–11] Due to the high frequency and low energy damping of MS waves, great efforts are being devoted to the manipulation of MS waves in order to use them in microwave communications. For example, the scattering obstacles for visible lights, such as fog, clouds, and smoke, are transparent for electromagnetic waves in the gigahertz range. The coupling of electromagnetic waves and MS excitations can generate high-frequency band-stop magnetic filters.[12] Very recently, to reduce size, weight, and cost of the microwave devices, there has been growing interest in exploring various multilayer structures.[13] Due to the fact that more structural parameters can be tuned in an aperiodic system compared to a periodic structure, it is interesting to investigate the propagation of MS waves in the aperiodic systems, such as Fibonacci multilayers,[14,15] and broaden their technological applications in several different fields.[16,17]

It is well known that there are bulk and surface/interface spin waves in dipolar magnetic multilayers, where the saturation magnetization lies parallel to the layers. If the in-plane propagation wave vector of the spin waves is restricted to be perpendicular to the saturation magnetization, one finds that a bulk wave in the multilayer is composed of surface waves within each layer, and the amplitude of these surface waves varies sinusoidally throughout the layers of the superlattices. While, a surface wave in the multilayer is composed of the surface wave within each layer, but the amplitude of the waves decreases exponentially as one penetrates into the superlattice. Therefore, in a multilayer system, spin waves are coupled to induce the collective excitation of the whole multilayer when the layer thickness is relatively thin. Since the MS coupling of different layers depends critically upon the structure of multilayers, it is interesting to investigate the spin waves in magnetic multilayers with different configurations, such as a Thue-Morse structure.

The Thue-Morse (TM) sequence is one of the well-known examples in one-dimensional (1D) aperiodic structure.[18] It contains two building blocks, A and B, and can be produced by repeating application of the substitution rules $A \rightarrow AB$ and $B \rightarrow BA$. It has been studied theoretically by Fourier spectra and electronic spectra of the Thue-Morse structures.[19] Very recently, resonant transmissions and omnidirectional reflections of electromagnetic waves have been found both theoretically and experimentally in a TM dielectric multilayer.[20] Here, we consider the magnetostatic excitation in a TM antiferromagnetic/nonmagnetic multilayer with Voigt geometry:[14] the magnetostatic spin waves propagate parallel to the surface of the film and perpendicular to the applied field along which the saturation magnetization exists. Based on the transfer-matrix method, the eigenfrequency spectra of MS waves and the profiles of precession amplitude of total magnetization are numerically obtained. The multiformity in frequency spectra may lead to a tunable magnetostatic wave.

II. THE THEORETICAL MODEL

A TM antiferromagnetic multilayer contains two building blocks, A and B. Each building block is constructed by

[a)]Author to whom correspondence should be addressed; electronic mail: rwpeng@nju.edu.cn

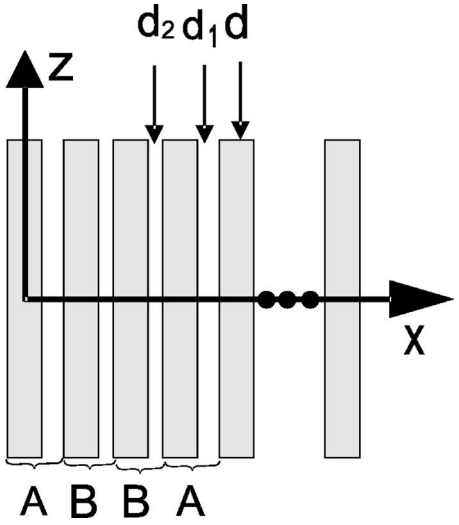

FIG. 1. The geometry of the Thue-Morse multilayer. The thickness of the antiferromagnetic layer is d and the thicknesses of the nonmagnetic spacer are d_1 and d_2 in blocks A and B, respectively.

one antiferromagnetic layer and one nonmagnetic layer. The antiferromagnetic layers in A and B blocks have the same thickness d, but the nonmagnetic layers have the thicknesses d_1 in A block and d_2 in B block. By repeated application of the substitution rules $A \rightarrow AB$ and $B \rightarrow BA$, the nth generation S_n of TM sequence can be obtained. For example, the first several generations are as follows:

$$S_0 = \{A\},$$

$$S_1 = \{AB\},$$

$$S_2 = \{ABBA\},$$

$$S_3 = \{ABBABAAB\},$$

$$S_4 = \{ABBABAABBAABABBA\}.$$

Now we concentrate on the magnetostatic excitation in the antiferromagnetic multilayer system. Suppose the growth of the multilayer is along the x direction, the wave vector along the y direction, and the easy axis along the z direction (as shown in Fig. 1). The two parts in the sublattice A (or B) are denoted by (I) and (II), respectively. The total magnetization in each sublattice can be treated as $m_i^T = m_i^{\mathrm{I}} + m_i^{\mathrm{II}}$ with $i = x, y$. The magnetostatic form of Maxwell's equations follows

$$\nabla \cdot \mathbf{B} = 0, \quad \nabla \times \mathbf{H} = 0, \tag{1}$$

with the constitutive relation $\mathbf{B} = \vec{\vec{\mu}}\mathbf{H}$, where $\vec{\vec{\mu}}$ is the permeability tensor. If the fluctuation field has the time dependence of $e^{-i\omega t}$, where ω is the frequency, $\vec{\vec{\mu}}$ takes the form

$$\vec{\vec{\mu}} = \begin{pmatrix} \mu_1 & i\mu_2 & 0 \\ -i\mu_2 & \mu_1 & 0 \\ 0 & 0 & 1 \end{pmatrix}, \tag{2}$$

for a uniaxial material. For an antiferromagnet, we have[5]

$$\mu_1 = 1 + \frac{4\pi\gamma^2 H_a M}{\omega_0^2 - (\omega + \gamma H_0)^2} + \frac{4\pi\gamma^2 H_a M}{\omega_0^2 - (\omega - \gamma H_0)^2}, \tag{3}$$

$$\mu_2 = \frac{4\pi\gamma^2 H_a M}{\omega_0^2 - (\omega + \gamma H_0)^2} - \frac{4\pi\gamma^2 H_a M}{\omega_0^2 - (\omega - \gamma H_0)^2}, \tag{4}$$

$$\omega_0 = \sqrt{\gamma^2 (2H_{\mathrm{ex}} H_a + H_a^2)}. \tag{5}$$

Here, H_0 is the external applied field, H_a is the anisotropy field, H_{ex} is the effective exchange field, M is the saturation magnetization of one of the sublattices, and γ is the gyromagnetic ratio. The quantity ω_0 is recognized as the antiferromagnetic resonance frequency in zero applied field.

In the magnetostatic limit, the magnetic scalar potential ϕ is introduced by $H = -\nabla\phi$. According to Eqs. (1) and (2), the scalar potential ϕ obeys the equation of motion given by

$$\mu_1 \left(\frac{\partial^2}{\partial x^2} + \frac{\partial^2}{\partial y^2} \right) \phi + \frac{\partial^2}{\partial z^2} \phi = 0, \tag{6}$$

in both the magnetic and nonmagnetic materials. Obviously, $\vec{\vec{\mu}} = \vec{\vec{1}}$ is in the nonmagnetic material. At the interface of layers, the continuum conditions require

$$\mu_1 \frac{\partial \phi^{\mathrm{in}}}{\partial x} - i\mu_2 \frac{\partial \phi^{\mathrm{in}}}{\partial y} = \frac{\partial \phi^{\mathrm{ex}}}{\partial x}, \tag{7}$$

$$\phi^{\mathrm{in}} = \phi^{\mathrm{ex}}, \tag{8}$$

where ϕ^{in} and ϕ^{ex} are the potentials inside the antiferromagnetic and nonmagnetic layers, respectively.

Following the work of Damon and Eshbach,[6] without loss of generation, we assume that only a plane wave e^{iky} propagates along the y direction with the in-plane wave vector k. It is reasonable to write $\phi = \varphi(x) e^{i(ky - \omega t)}$ for both antiferromagnetic and nonmagnetic layers. Equation (6) can be rewritten as

$$\left(\frac{d^2}{dx^2} - k^2 \right) \varphi(x) = 0. \tag{9}$$

The solution of Eq. (9) in the antiferromagnetic layers and nonmagnetic layers has the form

$$\varphi_l(x) = A_l e^{k(x - x_l)} + B_l e^{-k(x - xl)}, \tag{10}$$

$$\varphi_l(x) = C_l e^{k(x - x_l - d/2 - d_l/2)} + D_L e^{-k(x - x_l - d/2 - d_l/2)} \quad (i = 1,2), \tag{11}$$

respectively, where l denotes the block index and x_l is the intersection of midplanes of the lth antiferromagnetic layer with the x axis. Using Eqs. (7) and (8), the coefficients of A_l, B_l and A_{l+1},B_{l+1} of two adjacent antiferromagnetic layers are related to

$$\begin{pmatrix} A_{l+1} \\ B_{l+1} \end{pmatrix} = T(i) \begin{pmatrix} A_l \\ B_l \end{pmatrix}, \tag{12}$$

where $T(i)$ is a transfer matrix. In a Thue-Morse system, $T(i)$ has two different forms, $T(1)$ and $T(2)$, which satisfy

$$T(i) = \begin{pmatrix} T_{11}(i) & T_{12}(i) \\ T_{21}(i) & T_{22}(i) \end{pmatrix} \quad (i = 1,2), \tag{13}$$

where

$$T_{11}(i) = \{[(\mu_1+1)^2-\mu_2^2]e^{kd_i} - [(\mu_1-1)^2-\mu_2^2]e^{-kd_i}\}e^{kd}/(4\mu_1),$$

$$T_{12}(i) = (1+\mu_1-\mu_2)(1+\mu_2-\mu_1)(e^{kd_i}-e^{-kd_i})/(4\mu_1),$$

$$T_{21}(i) = (1+\mu_1+\mu_2)(1-\mu_2-\mu_1)(e^{-kd_i}-e^{kd_i})/(4\mu_1),$$

$$T_{22}(i) = \{[(\mu_1+1)^2-\mu_2^2]e^{-kd_i} - [(\mu_1-1)^2-\mu_2^2]e^{kd_i}\}e^{-kd}/(4\mu_1).$$

Obviously, $T(1)$ and $T(2)$ are unimodular.

Now we consider a case under a free-boundary condition. Suppose N is the total number of antiferromagnetic layers in the jth order of the TM multilayer. By exploiting Eqs. (7) and (8) at the two surfaces, we can obtain the following two equations:

$$(\mu_1+\mu_2-1)A_1 + (\mu_1-\mu_2-1)B_1e^{kd} = 0, \tag{14}$$

$$(\mu_1+\mu_2+1)A_N + (\mu_1-\mu_2+1)B_Ne^{-kd} = 0. \tag{15}$$

Meanwhile, the global equation for a TM multilayer can be written as

$$\begin{pmatrix} A_N \\ B_N \end{pmatrix} = M_j \begin{pmatrix} A_1 \\ B_1 \end{pmatrix}, \tag{16}$$

where $M_j = \begin{pmatrix} m_{11} m_{12} \\ m_{21} m_{22} \end{pmatrix}$ is a global transfer matrix. The linear equations (14)–(16) have a nontrivial solution only if the determinant of the coefficient vanishes. Therefore, we can obtain the recursion equation as follows:

$$[\mu_1^2-(\mu_2+1)^2]e^{kd}m_{11} - [(\mu_1+\mu_2)^2-1]m_{12} + [(\mu_1-\mu_2)^2-1]m_{21} - [\mu_1^2-(\mu_2-1)^2]e^{-kd}m_{22} = 0. \tag{17}$$

Obviously, the physical properties of magnetostatic excitations of the TM multilayer are decided by the dispersion relation (17).

Besides, the procession of total magnetization in the TM multilayer can be also obtained from the transfer-matrix method. According to the work of Grünberg and Mika,[2] the profiles of procession amplitudes m_x and m_y of total magnetization in the lth antiferromagnetic layers can be written as

$$m_x = \frac{1}{4\pi}[(\mu_1+\mu_2-1)A_le^{k(x-x_l)} + (\mu_2-\mu_1+1)B_le^{-k(x-x_l)}], \tag{18}$$

$$m_y = \frac{1}{4\pi}[(\mu_1+\mu_2-1)A_le^{k(x-x_l)} - (\mu_2-\mu_1+1)B_le^{-k(x-x_l)}]. \tag{19}$$

Here the coefficients A_l and B_l can be deduced from Eq. (16).

III. NUMERICAL CALCULATIONS AND DISCUSSION

Based on the above theoretical analysis, we can obtain the eigenfrequency spectra of the magnetostatic excitation for a TM system. In the following numerical calculation, we choose MnF_2 as the antiferromagnetic material with the Néel temperature around 67 K. The magnetic parameters[5] are as follows: the exchange field $H_{ex}=55$ T, the anisotropy field $H_a=0.787$ T, the external field $H_0=200$ Oe, and the sublattice magnetization $M=600$ G. Figure 2 shows the eigenfrequency of the TM superlattices as a function of the generation number. Actually, only if μ_1 is negative, Eq. (17) has a real solution and the magnetostatic excitation occurs. Therefore, the eigenfrequency of magnetostatic wave should satisfy $\omega_0-\gamma H_0<\omega<(\omega_0^2+8\pi\gamma^2H_aM)^{1/2}+\gamma H_0$. It is shown that the frequency spectrum of the TM superlattice contains two branches: ω_+ and ω_-, respectively. The gap between two branches, ω_+ and ω_-, is dependent of the external field. With increasing the external field H_0, the branch ω_+ moves upwards and the branch ω_- moves downwards. Therefore, the gap becomes larger [as shown in Fig. 2(a)]. Moreover, in each branch (ω_+ or ω_-), by increasing the generation number, separated modes gradually form the band [as shown in Fig. 2(b)]. Thereafter, more and more subbands and gaps emerge [as shown in Fig. 2(b)]. The number of subbands in each branch (ω_+ or ω_-) is $F_j=2^j$. The whole eigenfrequency spectrum presents a cantorlike behavior.

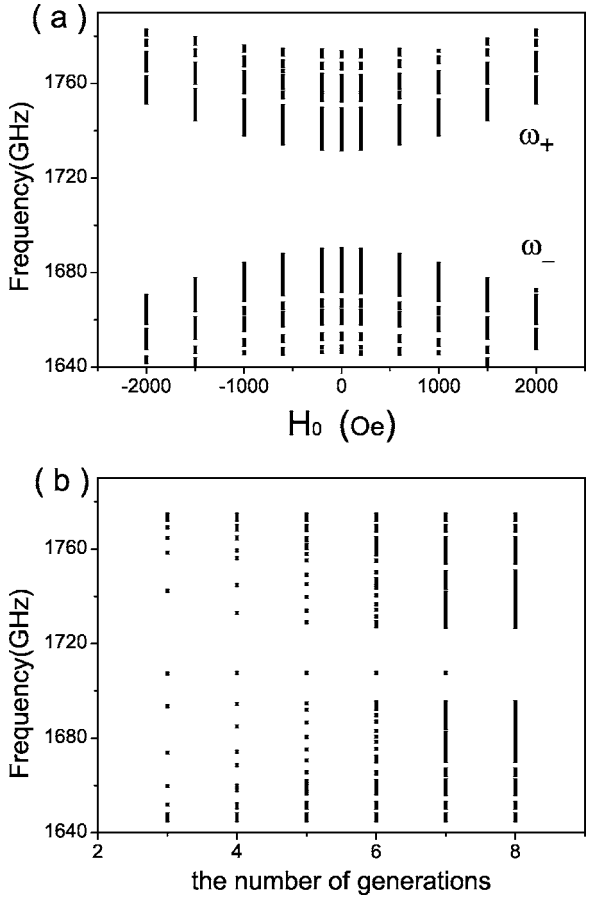

FIG. 2. (a) The eigenfrequency spectrum of the magnetostatic wave in the eight TM multilayer as a function of the external field H_0. (b) The eigenfrequency spectrum of the magnetostatic wave in the Thue-Morse multilayers with the generation number j. In each multilayer, $kd=0.5$, $kd_1=\frac{3}{4}kd$, and $kd_2=\frac{1}{4}kd$. ω_+ band is up and ω_- band is below.

Figure 3(a) shows the dispersion relation of magnetostatic modes for eight order TM multilayers with $kd=4kd_2$ and $kd_1=3kd_2$. It is shown that the two branches ω_+ and ω_-

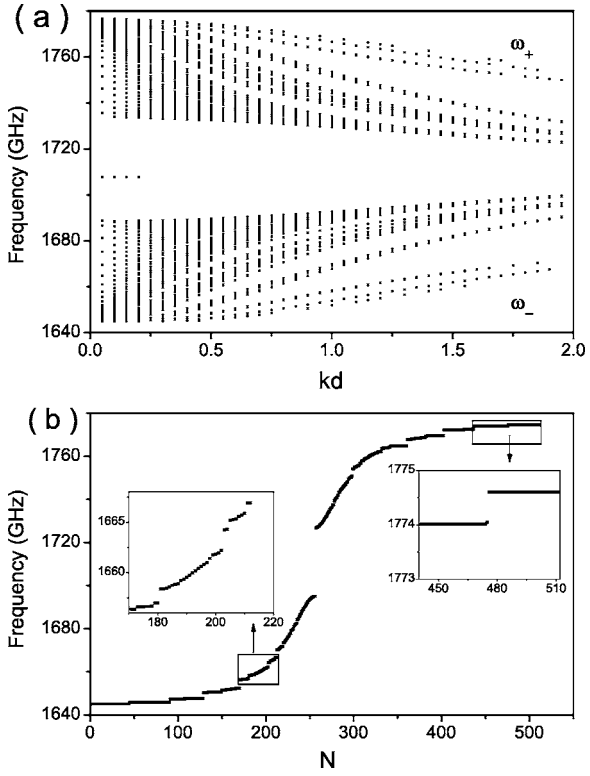

FIG. 3. (a) Dispersion relation of the eigenfrequency for the eight order TM multilayers with $kd_2=\frac{1}{4}kd$ and $kd_1=\frac{3}{4}kd$. (b) Eigenfrequency vs the number of modes for the eight order TM multilayers with $kd=0.5$, $kd_1=0.375$, and $kd_2=0.125$. Two enlarged local regions are shown in the insets.

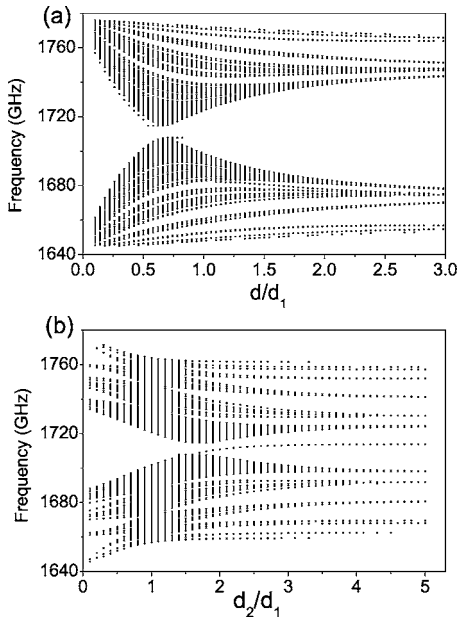

FIG. 4. The eigenfrequency distribution with the thickness ratio. (a) d/d_1 when $kd_1=0.6$ and $kd_2=0.2$. (b) d_2/d_1 for $kd=0.8$ and $kd_1=0.6$.

are separated by a gap as in the periodic multilayer. Each branch consists of bandlike dense modes and "isolated" modes in the gaps. The modes are highly degenerated with kd increasing. For the intermediate value of kd, the subbands are most obvious and hence the effect of nonperiodicity in the structure is strongest. As kd decreases, the band becomes relatively uniform and the feature of nonperiodicity is not obvious. In order to understand the frequency distribution of states in detail, we calculate the eigenfrequencies of the TM multilayer with $N=512$, $kd=0.5$, $kd_1=0.375$, and $kd_2=0.125$, as shown in Fig. 3(b). In Fig. 3(b), the allowed frequency forms two branches which are singularly continuous. The magnetostatic modes in each branch present both trifurcation and bifurcation, as shown in the insets of Fig. 3(b). This property is similar to the electronic behavior in the TM structure.[21]

The magnetostatic modes in the TM structures also depend on the thickness ratio of the antiferromagnetic layer and the nonmagnetic layer in the multilayer. Figure 4 shows the eigenfrequency distribution with different thickness ratios of the antiferromagnetic (AF) layer and the nonmagnetic (NM) layer. With increasing the thickness ratio d/d_1, the whole band is separated into two, three, or four subbands [as shown in Fig. 4(a)]. While with increasing the thickness ratio d_2/d_1, more subbands are found [as shown in Fig. 4(b)]. Note that there are obviously two continuous band for $d_2/d_1=1$, where the structure becomes periodic. However, for small or large values of d_2/d_1, the nonperiodicity of the structure becomes prominent, which leads to the diversity of the frequency spectrum of magnetostatic excitations in the TM multilayers. This property makes it possible to obtain the magnetostatic wave at the desired frequencies by designing some special structures and also to achieve the tunable devices of magnetostatic wave.

In order to describe the property of the magnetostatic modes, we have calculated the precession amplitudes m_x and m_y of magnetization in the TM multilayer. The profiles of total magnetization were numerically obtained at each antiferromagnetic layer. Three types of magnetostatic modes in the finite system are found: extended states, critical states, and localized states. First, for the frequencies in the band, some states of magnetostatic modes are extended, as shown in Figs. 5(a)–5(d). Figure 5 shows the distribution of precession amplitudes at each antiferromagnetic layer of the TM multilayers with the generation number $j=8$ and the total number of layers $N=256$. It can be seen that aperiodic amplitudes are modulated by a sine-like wave. Thus the system behaves mainly like an ordinary periodic multilayer. As frequency increases from the edge of the band, the modulation wavelength decreases approximately following the relation $\lambda=2D/n$ $(n=1,2,3,\ldots,)$, where D is the total thickness of the multilayer. This behavior is very similar to the case of periodic magnetic multilayers. Second, for the modes in the subband, most states of magnetostatic modes are critical, as shown in Figs. 6(a)–6(d). The distribution of magnetization is neither sine-like extended nor an exponential decay, but it is critical. Third, for the modes at the edge of the band or in the gap, the states of magnetostatic modes are localized, as shown in Figs. 7(a)–7(d). Figures 7(a) and 7(b) show one kind of surface modes in the TM multilayers. The amplitude of the surface mode is oscillating and damping from the surface. While, the modes shown in Figs. 7(c) and 7(d) are another surface mode of the multilayers, whose amplitude decays exponentially from a surface. This mode is similar to the DE surface mode of a single magnetic layer with thickness Nd. Anyway, the frequency of the precession in the TM

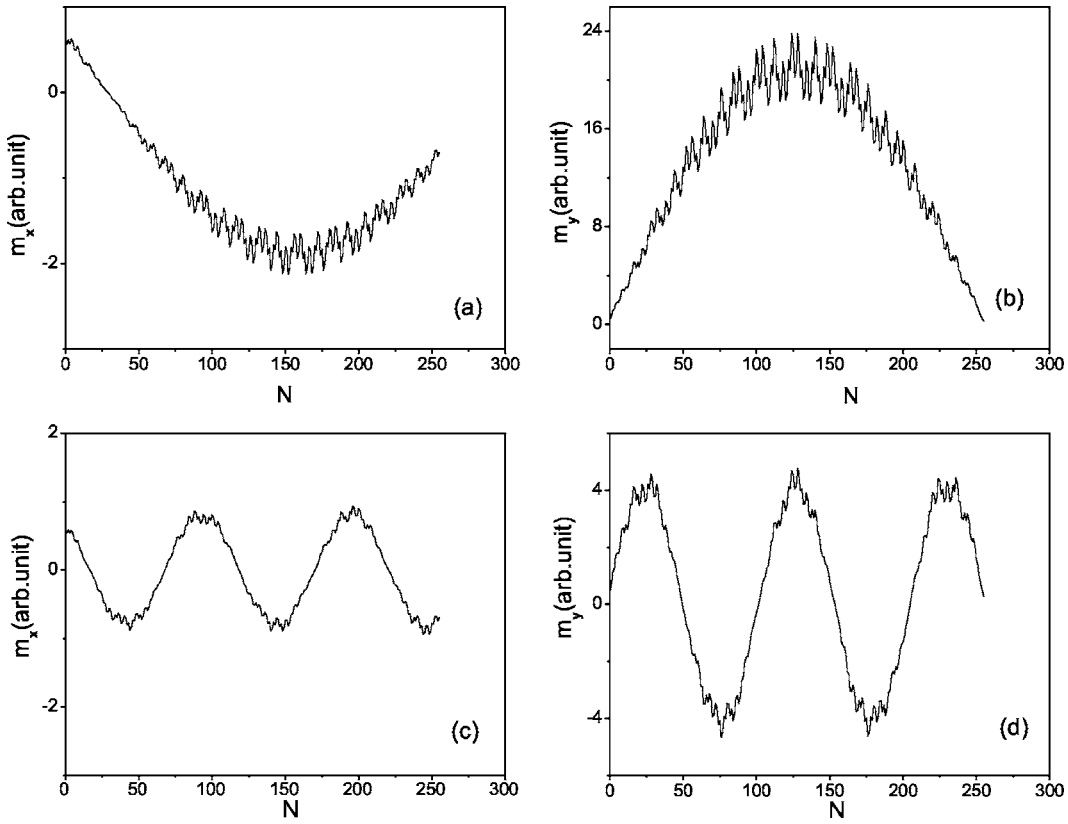

FIG. 5. The profiles of total magnetization are extended for the eigenfrequency near the top edge of the band. Here $kd=0.5$, $kd_1=\frac{3}{4}kd$, and $kd_2=\frac{1}{4}kd$. (a) m_x and (b) m_y at $\omega=17\,324\,022\,806$ Hz; (c) m_x and (d) m_y at $\omega=1\,732\,910\,615\,218$ Hz.

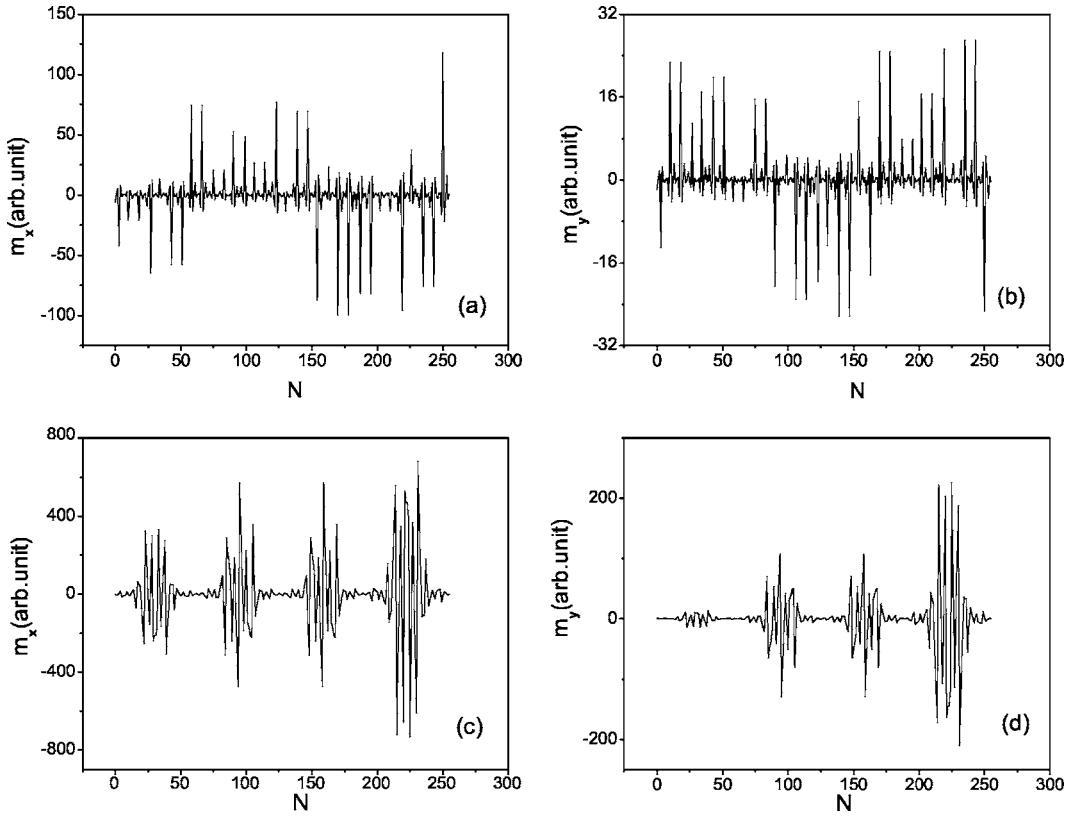

FIG. 6. The profiles of total magnetization are critical for the eigenfrequency in the band. Here $kd=1.0$, $kd_1=\frac{3}{4}kd$, and $kd_2=\frac{1}{4}kd$. (a) m_x and (b) m_y at $\omega=1\,766\,461\,220\,041$ Hz. (c) m_x and (d) m_y at $\omega=1\,751\,822\,684\,543$ Hz.

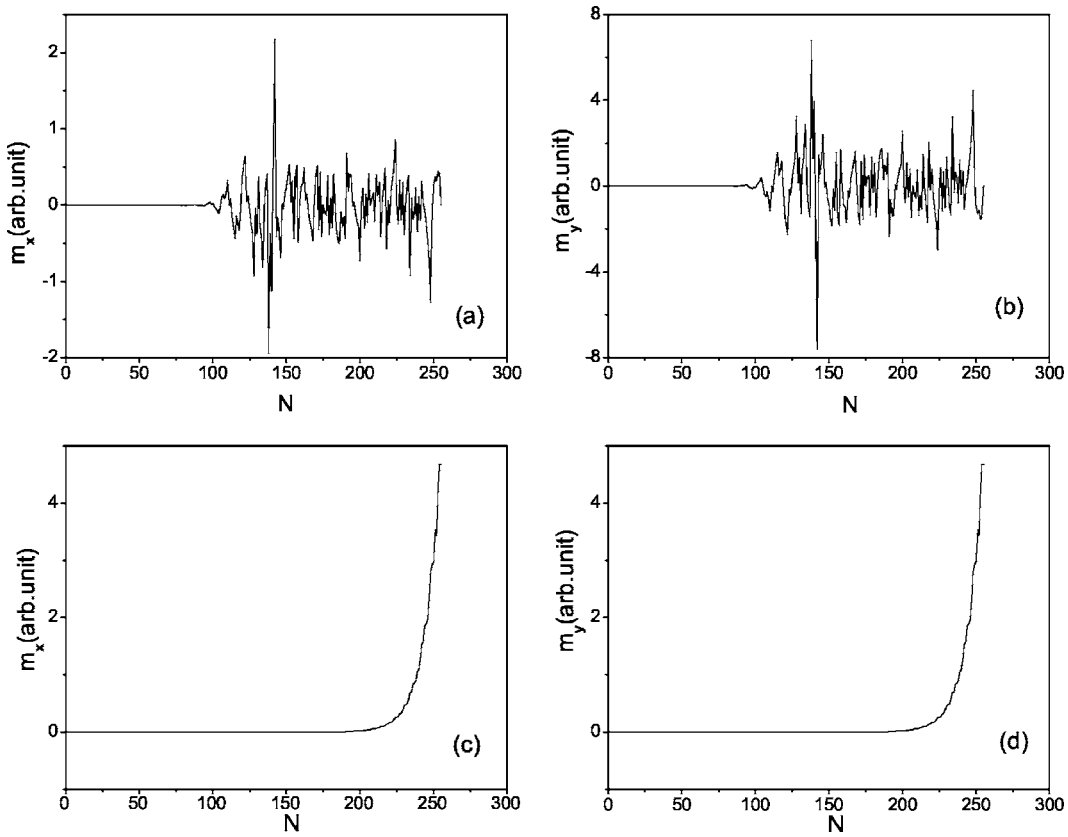

FIG. 7. The profiles of total magnetization are localized for the eigenfrequency at the edge of the band or in the gap. Here $kd_1=\frac{3}{4}kd$ and $kd_2=\frac{1}{4}kd$. (a) m_x and (b) m_y when $kd=1.0$ and $\omega=1\,685\,218\,100\,350$ Hz. (c) m_x and (d) m_y when $kd=0.2$ and $\omega=1\,707\,639\,949\,363$ Hz.

multilayer is sensitive to the structure, the thickness of the AF and NM layers, and the external applied field.

IV. SUMMARY

In this work, we have theoretically studied the magnetostatic excitation in Thue-Morse (TM) antiferromagnetic/nonmagnetic multilayers. Based on the transfer-matrix method, the dispersion relation of magnetostatic spin waves and the precession amplitude of the total magnetization have been obtained. Two bands of dual structures are found in the frequency spectra and the hierarchical feature is presented in each subband. The states in the finite system can be categorized to three types: extended states in the band, critical states in the subband, and localized surface states in the gaps. The frequency spectrum depends on the external applied filed, the TM structure, and the layer thickness. The multiformity in frequency spectra leads to a tunable magnetostatic wave, which may have potential applications in designing devices of MS waves for microwave communications.

ACKNOWLEDGMENTS

This work was supported by the grants from National Natural Science Foundation of China (10374042, 10021001, 90201039, and 10374043), the State Key Program for Basic Research from the Ministry of Science and Technology of China (2004CB619005), NSF of Jiangsu, China (BK2004209), and partly by the Ministry of Education of China (NCET-05-0440) and Fok Ying Tung Education Foundation.

[1] R. E. Camley, T. S. Rahman, and D. L. Mills, Phys. Rev. B **27**, 261 (1983).
[2] P. Grünberg and K. Mika, Phys. Rev. B **27**, 2955 (1983).
[3] C. Mathieu, M. Bauer, B. Hillebrands, J. Fassbender, G. Güntherodt, R. Jungblut, J. Kohlhepp, and A. Reinders, J. Appl. Phys. **83**, 2863 (1999).
[4] B. Luthi, D. L. Mill, and R. E. Camley, Phys. Rev. B **28**, 1475 (1983).
[5] R. E. Camley and M. G. Cottam, Phys. Rev. B **35**, 189 (1987).
[6] R. W. Damon and J. R. Eshbach, J. Phys. Chem. Solids **19**, 308 (1961).
[7] S. S. P. Parkin, Phys. Rev. Lett. **67**, 3598 (1991).
[8] P. Grunberg, R. Schreiber, Y. Pang, M. B. Brodsk, and H. Sowers, Phys. Rev. Lett. **57**, 2442 (1986).
[9] J. Kwo, M. Hong, F. J. Disalvo, J. V. Waszczak, and C. F. Majkrzak, Phys. Rev. B **35**, 7295 (1987).
[10] A. Ghosh and S. N. Karmakar, Phys. Rev. B **58**, 2586 (1998).
[11] E. L. Albuquerque, R. N. Costa Filho, and M. G. Cottam, J. Appl. Phys. **87**, 5398 (2000).
[12] B. Kuanr, Z. Celinski, and R. E. Camley, Appl. Phys. Lett. **83**, 3969 (2003).
[13] B. K. Kuanr, D. L. Marvin, T. M. Christensen, R. E. Camely, and Z. Celinski, Appl. Phys. Lett. **87**, 222506 (2005).
[14] J. W. Feng, G. J. Jin, A. Hu, S. S. Jiang, and D. Feng, Phys. Rev. B **52**, 15312 (1995).
[15] S. S. Kang, Phys. Rev. B **65**, 064401 (2002).
[16] E. Die, F. Dominguez-Adame, E. Macia, and A. Sanchez, Phys. Rev. B **54**, 16792 (1996); E. Macia, Appl. Phys. Lett. **73**, 3330 (1998).
[17] R. W. Peng, X. Q. Huang, F. Qiu, M. Wang, A. Hu, and S. S. Jiang, Appl. Phys. Lett. **80**, 3063 (2002); R. W. Peng, M. Mazzer, and K. W. J. Barnham, *ibid.* **83**, 770 (2003).
[18] R. Riklund and M. Severin, J. Phys.: Condens. Matter **21**, 3217 (1998); M. Dulea, M. Severin, and R. Riklund, Phys. Rev. B **42**, 3680 (1990).

[19]C. Godreche and J. M. Luck, J. Phys. A **23**, 3769 (1990); M. G. Qin, H. R. Ma, and C. H. Tsai, J. Phys.: Condens. Matter **2**, 1059 (1990); A. Bovier and J. Ghez, J. Phys. A **28**, 2313 (1995); S. Chattopadhyay and A. Chakrabarti, J. Phys.: Condens. Matter **12**, 5681 (2000).

[20]F. Qiu, R. W. Peng, X. Q. Huang, Y. M. Liu, M. Wang, A. Hu, and S. S. Jiang, Europhys. Lett. **63**, 853 (2003); F. Qiu, R. W. Peng, X. Q. Huang, X. F. Hu, M. Wang, A. Hu, S. S. Jiang, and D. Feng, *ibid.* **68**, 658 (2004).

[21]S. F. Cheng and G. J. Jin, Phys. Rev. B **65**, 134206 (2002).